

Factors Affecting the Strength of X–H···H–M Hydrogen Bonds

Eduardo Peris,[†] Jesse C. Lee, Jr.,[†] Joe R. Rambo,[‡] Odile Eisenstein,^{*,‡} and Robert H. Crabtree^{*,†}

Contribution from the Department of Chemistry, Yale University, 225 Prospect Street, New Haven, Connecticut 06511, and Laboratoire de Chimie Théorique, Université de Paris-Sud, 91407 Orsay, France

Received October 14, 1994[⊗]

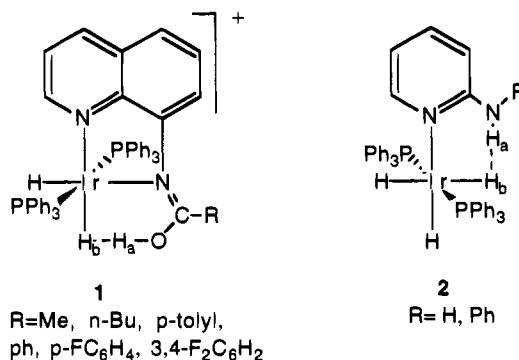
Abstract: The strengths of intramolecular H···H and H···Y hydrogen bonding between a ligating 2-aminopyridine NH group and a cis Ir–H bond or a cis halo group has been estimated (1.8–5.2 kcal/mol) in a series of compounds of general form $[\text{IrH}_2(\text{Y})(2\text{-C}_6\text{H}_4\text{NH}_2)(\text{PPh}_3)_2]^{n+}$ (Y = H[−], F[−], Cl[−], Br[−], I[−], SCN[−], and CN[−], n = 0, and Y = CO and MeCN, n = 1) by a new method involving measuring the Ar–NH₂ rotation barrier by ¹H NMR. The H-bonding interaction is surprisingly strong; in cases where both are possible, N–H···H–Ir hydrogen bonding is preferred over N–H···Cl–Ir H-bonding. The experimental barrier for C–N bond rotation in $[\text{IrH}_2(\text{Y})(2\text{-C}_6\text{H}_4\text{NH}_2)(\text{PPh}_3)_2]^{n+}$ was in the range 7.6–11.0 kcal/mol, as determined by ¹H NMR. From a simple geometrical study it appears that the two H-bonded hydrogens can approach appropriately close to each other. In contrast, the geometry of the situation is not as favorable for N–H···Y–Ir H-bonding for Y = F[−], Cl[−], Br[−], and I[−]. From core potential ab initio studies, the H-bond strength was estimated to be in the range 5.7–7.1 kcal/mol, assuming that the intrinsic C–N rotation barrier is the same in free and coordinated 2-C₆H₄NH₂. These unusual hydrogen bonds (A–H···B) are proposed to be strong for an element B having the electronegativity of hydrogen because of (i) a favorable geometry which allows NH and IrH to approach very close to one another and (ii) the facility with which Ir–H may be polarized in the sense Ir^{δ+}–H^{δ−} on the approach of the N–H bond. The calculations also suggest that the reason changing the nature of the ligand Y trans to the H-bonded Ir–H group alters the strength of the H-bond is that the δ[−] charge on the Ir–H is affected. The higher the trans effect of Y, the higher the δ[−] charge and the stronger the NH···Hr bonding interaction.

Introduction

The great importance of hydrogen bonding has long been recognized.^{1–5} Typically, a weak acid, A–H, interacts with the lone pair of a weak base, B, where A and B are electronegative atoms such as nitrogen, oxygen, and the halogens; the strength of the interaction is normally on the order of 3–15 kcal/mol.

It has recently been shown that O–H and N–H bonds can act as the weak acid component, AH, toward metals,^{3,4,7} M, or M–H bonds^{5,6} as the weak base component, B. Examples of

the second type are **1** and **2**.⁶ Characteristic of these systems



are H_a···H_b coupling constants of 2–5 Hz in the proton NMR, a large excess relaxation of H_a and H_b indicating an H_a···H_b distance of ca. 1.8 Å, and the low field shift of the X–H proton resonance (X = O or N). Special features of this system which have been proposed^{6b} to lead to the strong interaction include (i) the ability of H_a and H_b to approach very close to one another, (ii) the absence of lone pairs on the Ir–H proton, and (iii) the facility with which Ir–H_b may be polarized on the approach of the X–H group.

In this paper we report some new examples of this phenomenon in which the system is designed so as to allow the strength of the hydrogen bond to be estimated. Further, ab initio studies of model complexes support the significance of this interaction.

* To whom correspondence should be addressed.

[†] Yale University.

[‡] Université de Paris-Sud.

[⊗] Abstract published in *Advance ACS Abstracts*, March 1, 1995.

(1) (a) Jeffrey, G. A.; Saenger, W. *Hydrogen Bonding in Biological Structures*; Springer: New York, 1991. (b) Schuster, P.; Zundel, G., Sandorfy, C., Eds. *The Hydrogen Bond*; North-Holland: Amsterdam, New York, Oxford, 1976.

(2) Hadzi, D., Ed. *Hydrogen Bonding*; Pergamon: New York, 1959.

(3) Brammer, L.; Zhao, D. *Organometallics* **1994**, *13*, 1545.

(4) Brammer, L.; Charnock, J. M.; Goggin, P. L.; Goodfellow, R. J.; Orpen, A. G.; Koetzle, T. F. *J. Chem. Soc., Dalton Trans.* **1991**, 1789.

(5) (a) Lough, A. J.; Park, S.; Ramachandran, R.; Morris, R. H. *J. Am. Chem. Soc.* **1994**, *116*, 8356. (b) Ramachandran, R.; Morris, R. H. *J. Chem. Soc., Chem. Commun.* **1994**, 2201.

(6) (a) Lee, C. J., Jr.; Rheingold, A. L.; Muller, B.; Pregosin, P. S.; Crabtree, R. H. *J. Chem. Soc., Chem. Commun.* **1994**, 1021. (b) Lee, C. J., Jr.; Peris, E.; Rheingold, A. L.; Crabtree, R. H. *J. Am. Chem. Soc.* **1994**, *116*, 11014.

(7) Stevens, R. C.; Bau, R.; Milstein, D.; Blum, O.; Koetzle, T. F. *J. Chem. Soc., Dalton Trans.* **1990**, 1429.

Experimental Section

General Procedures and Materials. $[\text{IrH}_2(\text{Me}_2\text{CO})_2(\text{PPh}_3)_2]\text{BF}_4$ and $\text{IrH}_5(\text{PPh}_3)_2$ were obtained according to literature methods.^{8,9} All solvents were of analytical grade and were degassed before use. All reactions were run under N_2 . Ligands were used as received. NMR measurements were recorded on a GE Omega-300 or QE300-plus spectrometer. IR spectra were recorded on a MIDAC M1200 Model FTIR. Kinetic data were measured by ^1H NMR spectroscopy according to the excess bandwidth and coalescence temperature methods.¹⁰

Synthesis of Compounds. Dihydrido(η^2 -2-oxypyridine)bis(triphenylphosphine)iridium(III) (3). $[\text{IrH}_5(\text{PPh}_3)_2]$ (20 mg, 0.028 mmol) and 2-hydroxypyridine (2.6 mg, 0.028 mmol) were warmed to 80 °C in benzene (20 mL) for 5 min. The solvent was removed *in vacuo* and the product recrystallized from CH_2Cl_2 -hexane (1:1, 5 mL) to give **3** (75%). ^1H NMR (CD_2Cl_2) (ppm) at 293 K: -29.7 [1H, td, $^2J(\text{HH}) = 9.5$ Hz, $^2J(\text{PH}) = 15.1$ Hz, IrH], -21.5 [1H, td, $^2J(\text{HH}) = 9.5$ Hz, $^2J(\text{PH}) = 15.1$ Hz, IrH], 5.1-6.9 [4H, m, $\text{C}_5\text{H}_4\text{N}$], 7.0-8.2 [30H, m, aromatics]. $^{31}\text{P}\{^1\text{H}$ selectively decoupled} NMR (CD_2Cl_2) (ppm): 22.8 [t, $^2J(\text{PH}) = 16$ Hz]. IR (film) (cm^{-1}): 2173 [br, IrH]. Anal. Calcd for $\text{IrP}_2\text{ONC}_4\text{H}_8$: C, 60.51; H, 4.67; N, 1.72. Found: C, 60.47; H, 4.82; N, 1.87.

Dihydridohalo(η^1 -2-hydroxypyridine)bis(triphenylphosphine)iridium(III) 4. $[\text{IrH}_2(\text{Me}_2\text{CO})_2(\text{PPh}_3)_2]\text{BF}_4$ (20 mg, 0.022 mmol), 2-hydroxypyridine (2.1 mg, 0.022 mmol), and Bu_4NY (0.022 mmol; $\text{Y} = \text{Cl}^-$, Br^- , I^-) were dissolved in 5 mL of CH_2Cl_2 and stirred at room temperature for 5 min. The resulting pale yellow solution was transferred to a chromatography column (0.5 × 10 cm) packed with silica gel in hexane. Elution with CH_2Cl_2 -hexane (10:1) afforded a single pale yellow band which was collected. The solvent was removed under vacuum, and the crude solid was recrystallized from 3 mL of CH_2Cl_2 -hexane (1:1) to give solid **4** as a mixture of isomers (**4H** and **4Y**) which was stored in a drying tube under vacuum for 36 h.

$\text{Y} = \text{Cl}^-$. (**4H**) ^1H NMR (CD_2Cl_2) (ppm): -21.8 [1H, tdd, $^2J(\text{HH}) = 4.2$ Hz, $^2J(\text{PH}) = 18.1$ Hz, $J(\text{HH}) = 5.5$ Hz, IrH], -19.9 [1H, td, $^2J(\text{HH}) = 4.2$ Hz, $^2J(\text{PH}) = 17.9$ Hz, IrH], 5.2-6.8 [4H, m, $\text{C}_5\text{H}_4\text{N}$], 7.0-7.9 [30H, m, aromatics], 9.5 [1H, d, $J(\text{HH}) = 5.5$ Hz, OH]. $^{31}\text{P}\{^1\text{H}$ selectively decoupled} NMR (CD_2Cl_2) (ppm): 18.5 [t, $^2J(\text{PH}) = 17$ Hz]. (**4Y**) ^1H NMR (CD_2Cl_2) (ppm): -23.6 [1H, td, $^2J(\text{HH}) = 4.6$ Hz, $^2J(\text{PH}) = 17.1$ Hz, IrH], -22.7 [1H, td, $^2J(\text{HH}) = 4.6$ Hz, $^2J(\text{PH}) = 17.2$ Hz, IrH], 5.2-6.8 [4H, m, $\text{C}_5\text{H}_4\text{N}$], 7.0-7.9 [30H, m, aromatics], 11.5 [1H, OH]. $^{31}\text{P}\{^1\text{H}$ selectively decoupled} NMR (CD_2Cl_2) (ppm): 23.1 [t, $^2J(\text{PH}) = 17$ Hz]. Anal. Calcd for $\text{IrP}_2\text{ONClC}_4\text{H}_8$: C, 57.97; H, 4.36; N, 1.65. Found: C, 57.68; H, 4.56; N, 1.82. IR (film) (cm^{-1}) (mixture of **4Y** and **4H**): 2175 [m, br, IrH], 3388 [m, br, OH].

$\text{Y} = \text{Br}^-$. (**4H**) ^1H NMR (CD_2Cl_2) (ppm): -21.0 [1H, tdd, $^2J(\text{HH}) = 4.3$ Hz, $^2J(\text{PH}) = 17.6$ Hz, $J(\text{HH}) = 5.4$ Hz, IrH], -20.1 [1H, td, $^2J(\text{HH}) = 4.3$ Hz, $^2J(\text{PH}) = 17.5$ Hz, IrH], 5.3-6.9 [4H, m, $\text{C}_5\text{H}_4\text{N}$], 7.0-7.8 [30H, m, aromatics], 9.5 [1H, d, $J(\text{HH}) = 5.4$ Hz, OH]. $^{31}\text{P}\{^1\text{H}$ selectively decoupled} NMR (CD_2Cl_2) (ppm): 17.8 [t, $^2J(\text{PH}) = 17.5$ Hz]. (**4Y**) ^1H NMR (CD_2Cl_2) (ppm): -22.9 [1H, td, $^2J(\text{HH}) = 4.6$ Hz, $^2J(\text{PH}) = 17.3$ Hz, IrH], -22.4 [1H, td, $^2J(\text{HH}) = 4.6$ Hz, $^2J(\text{PH}) = 17.2$ Hz, IrH], 5.3-6.9 [4H, m, $\text{C}_5\text{H}_4\text{N}$], 7.0-7.8 [30H, m, aromatics], 10.5 [1H, OH]. $^{31}\text{P}\{^1\text{H}$ selectively decoupled} NMR (CD_2Cl_2) (ppm): 23.1 [t, $^2J(\text{PH}) = 17$ Hz]. Anal. Calcd for $\text{IrP}_2\text{ONBrC}_4\text{H}_8(\text{CH}_2\text{Cl}_2)$: C, 51.53; H, 3.98; N, 1.43. Found: C, 51.61; H, 4.17; N, 1.32. IR (film) (cm^{-1}) (mixture of **4Y** and **4H**): 2184 [m, br, IrH], 3364 [w, br, OH].

$\text{Y} = \text{I}^-$. (**4H**) ^1H NMR (CD_2Cl_2) (ppm): -21.1 [1H, td, $^2J(\text{HH}) = 4.5$ Hz, $^2J(\text{PH}) = 17.6$ Hz, IrH], -18.9 [1H, tdd, $^2J(\text{HH}) = 4.5$ Hz, $^2J(\text{PH}) = 17.7$ Hz, $J(\text{HH}) = 5.7$ Hz, IrH], 5.2-6.8 [4H, m, $\text{C}_5\text{H}_4\text{N}$], 7.0-7.9 [30H, m, aromatics], 9.5 [1H, $J(\text{HH}) = 5.7$ Hz, OH]. $^{31}\text{P}\{^1\text{H}$ selectively decoupled} NMR (CD_2Cl_2) (ppm): 16.1 [t, $^2J(\text{PH}) = 17.5$ Hz]. Anal. Calcd for $\text{IrP}_2\text{ONIC}_4\text{H}_8$: C, 52.33; H, 3.93; N, 1.49.

Found: C, 52.45; H, 4.10; N, 1.57. IR (film) (cm^{-1}): 2181 [m, br, IrH].

Dihydridohalo(η^1 -2-(aminophenyl)pyridine)bis(triphenylphosphine)iridium(III) 6Y and 6H. $[\text{IrH}_2(\text{Me}_2\text{CO})_2(\text{PPh}_3)_2]\text{BF}_4$ (20 mg, 0.022 mmol), 2-(aminophenyl)pyridine (3.7 mg, 0.022 mmol), and Bu_4NY (0.022 mmol; $\text{Y} = \text{F}^-$, Cl^- , Br^- , I^-) were dissolved in 5 mL of CH_2Cl_2 and stirred at room temperature for 2 min. The pale yellow solution was transferred to a chromatography column and purified as described above.

$\text{Y} = \text{F}^-$. (**6Y**) ^1H NMR (CD_2Cl_2) (ppm) at 293 K: -30.55 [1H, br d, $^2J(\text{FH}) = 84.0$ Hz, IrH], -21.6 [1H, br, IrH], 5.5-8.2 [34H, aromatics and $\text{C}_5\text{H}_4\text{N}$], 11.9 (1H, d, $^2J(\text{FH}) = 65.1$ Hz). $^{31}\text{P}\{^1\text{H}$ selectively decoupled} NMR (CD_2Cl_2) (ppm): 23.0 (br). IR (film) (cm^{-1}): 2167 [m, br, IrH], 3181 [w, br, NH].

$\text{Y} = \text{Cl}^-$. (**6H**) ^1H NMR (CD_2Cl_2) (ppm): -22.7 [1H, td, $^2J(\text{HH}) = 4.7$ Hz, $^2J(\text{PH}) = 14.7$ Hz, IrH], -21.3 [1H, td, $^2J(\text{HH}) = 4.7$ Hz, $^2J(\text{PH}) = 14.9$ Hz, IrH], 5.2-7.9 [34H, m, aromatics and $\text{C}_5\text{H}_4\text{N}$], 8.6 [1H, NH]. $^{31}\text{P}\{^1\text{H}$ selectively decoupled} NMR (CD_2Cl_2) (ppm): 17.9 [t, $^2J(\text{PH}) = 14.7$ Hz]. (**6Y**) ^1H NMR (CD_2Cl_2) (ppm): -23.7 [2H, m, AB system, IrH], 5.2-7.9 [34H, m, aromatics and $\text{C}_5\text{H}_4\text{N}$], 10.4 [1H, NH]. $^{31}\text{P}\{^1\text{H}$ selectively decoupled} NMR (CD_2Cl_2) (ppm): 21.7 [t, $^2J(\text{PH}) = 14.8$ Hz]. Anal. Calcd for $\text{IrP}_2\text{N}_2\text{ClC}_4\text{H}_7\text{H}_2(\text{CH}_2\text{Cl}_2)$: C, 57.10; H, 4.36; N, 2.77. Found: C, 56.93; H, 4.40; N, 2.87. IR (film) (cm^{-1}) (mixture of **6Y** and **6H**): 2196 [m, br, IrH], 3185 [w, br, NH], 3260 [w, br, NH].

$\text{Y} = \text{Br}^-$. (**6H**) ^1H NMR (CD_2Cl_2) (ppm): -21.5 [1H, td, $^2J(\text{HH}) = 4.5$ Hz, $^2J(\text{PH}) = 15.5$ Hz, IrH], -21.2 [1H, td, $^2J(\text{HH}) = 4.5$ Hz, $^2J(\text{PH}) = 15.6$ Hz, IrH], 5.2-8.2 [34H, m, aromatics and $\text{C}_5\text{H}_4\text{N}$], 9.0 [1H, NH]. $^{31}\text{P}\{^1\text{H}$ selectively decoupled} NMR (CD_2Cl_2) (ppm): 17.9 [t, $^2J(\text{PH}) = 15.5$ Hz]. (**6Y**) ^1H NMR (CD_2Cl_2) (ppm): -23.5 [1H, td, $^2J(\text{HH}) = 4.4$ Hz, $^2J(\text{PH}) = 14.5$ Hz, IrH], -22.4 [1H, td, $^2J(\text{HH}) = 4.4$ Hz, $^2J(\text{PH}) = 14.6$ Hz, IrH], 5.2-8.2 [34H, m, aromatics and $\text{C}_5\text{H}_4\text{N}$], 8.2 [1H, NH]. $^{31}\text{P}\{^1\text{H}$ selectively decoupled} NMR (CD_2Cl_2) (ppm): 21.3 [t, $^2J(\text{PH}) = 14.6$ Hz]. IR (film) (cm^{-1}) (mixture of **6Y** and **6H**): 2190 [m, br, IrH], 3185 [w, br, NH], 3261 [w, br, NH].

$\text{Y} = \text{I}^-$. (**6H**) ^1H NMR (CD_2Cl_2) (ppm): -21.9 [1H, td, $^2J(\text{HH}) = 4.8$ Hz, $^2J(\text{PH}) = 14.5$ Hz, IrH], -21.2 [1H, td, $^2J(\text{HH}) = 4.8$ Hz, $^2J(\text{PH}) = 14.5$ Hz, IrH], 5.4-8.4 [34H, m, aromatics and $\text{C}_5\text{H}_4\text{N}$], 8.6 [1H, NH]. $^{31}\text{P}\{^1\text{H}$ selectively decoupled} NMR (CD_2Cl_2) (ppm): 16.1 [t, $^2J(\text{PH}) = 14.7$ Hz]. Anal. Calcd for $\text{IrP}_2\text{N}_2\text{IC}_4\text{H}_7\text{H}_2(\text{CH}_2\text{Cl}_2)$: C, 52.36; H, 4.00; N, 2.55. Found: C, 52.25; H, 3.49; N, 2.39. IR (film) (cm^{-1}): 2192 [m, br, IrH], 3195 [w, br, NH].

Dihydridohalo(η^1 -2-aminopyridine)bis(triphenylphosphine)iridium(III) 7Y and 7H. $[\text{IrH}_2(\text{Me}_2\text{CO})_2(\text{PPh}_3)_2]\text{BF}_4$ (20 mg, 0.022 mmol), 2-aminopyridine (2.1 mg, 0.022 mmol), and Bu_4NY (0.022 mmol; $\text{Y} = \text{F}^-$, Cl^- , Br^- , I^- , CN^- , SCN^-) were dissolved in 5 mL of CH_2Cl_2 and stirred at room temperature for 3 min. The yellow solution was transferred to a chromatography column and purified as described above.

$\text{Y} = \text{F}^-$. (**7Y**) ^1H NMR (CD_2Cl_2) (ppm) at 293 K: -29.6 [1H, dtd, $^2J(\text{HF}) = 79.8$ Hz, $^2J(\text{PH}) = 17.4$ Hz, $^2J(\text{HH}) = 8.4$ Hz, IrH], -21.6 [1H, tdd, $^2J(\text{PH}) = 21.0$ Hz, $^2J(\text{HH}) = 8.4$ Hz, $^2J(\text{FH}) = 3.6$ Hz, IrH], 5.2-7.0 (4H, $\text{C}_5\text{H}_4\text{N}$), 7.2-7.8 (30H, m, aromatics), 8.1 (2H, NH_2). ^1H NMR (CD_2Cl_2) (ppm) at 213 K: (same as that at 293 K except the NH_2 signal) 4.2 (1H, s, NH), 10.2 (1H, d, $^2J(\text{FH}) = 63.5$ Hz, NH). $T_c = 263$ K. $^{31}\text{P}\{^1\text{H}$ selectively decoupled} NMR (CD_2Cl_2) (ppm): 18.5 [t, $^2J(\text{PH}) = 21.0$ Hz]. Anal. Calcd for $\text{IrP}_2\text{N}_2\text{FC}_4\text{H}_8(\text{CH}_2\text{Cl}_2)$: C, 55.01; H, 4.37; N, 3.07. Found: C, 54.87; H, 4.45; N, 2.74. IR (film) (cm^{-1}): 2172, 2224 [m, br, IrH], 3324, 3433 [w, br, NH].

$\text{Y} = \text{Cl}^-$. (**7Y**) ^1H NMR (CD_2Cl_2) (ppm) at 293 K: -23.6 [1H, td, $^2J(\text{PH}) = 18.4$ Hz, $^2J(\text{HH}) = 6.4$ Hz, IrH], -23.6 [1H, td, $^2J(\text{PH}) = 18.2$ Hz, $^2J(\text{HH}) = 6.4$ Hz, IrH], 5.4-8.4 (34H, m, aromatics and $\text{C}_5\text{H}_4\text{N}$), 5.75 (2H, NH_2). $^{31}\text{P}\{^1\text{H}$ selectively decoupled} NMR (CD_2Cl_2) (ppm): 22.0 [t, $^2J(\text{PH}) = 18.2$ Hz]. (**7H**) ^1H NMR (CD_2Cl_2) (ppm) at 293 K: -22.9 [1H, td, $^2J(\text{PH}) = 19.4$ Hz, $^2J(\text{HH}) = 6.6$ Hz, IrH], -20.8 [1H, td, $^2J(\text{PH}) = 18.2$ Hz, $^2J(\text{HH}) = 6.6$ Hz, IrH], 5.4-8.4 (34H, m, aromatics and $\text{C}_5\text{H}_4\text{N}$), 5.25 (2H, s, NH_2). ^1H NMR (CD_2Cl_2) (ppm) at 183 K: (same as that at 293 K except the NH_2 signal) 4.6 (1H, s, NH), 6.2 (1H, s, NH). $T_c = 198$ K. $^{31}\text{P}\{^1\text{H}$ selectively decoupled} NMR (CD_2Cl_2) (ppm): 19.3 [t, $^2J(\text{PH}) = 18.2$ Hz]. IR

(8) Crabtree, R. H.; Demou, P. C.; Eden, D.; Mihelcic, J. M.; Parnell, C.; Quirk, J. M.; Morris, G. E. *J. Am. Chem. Soc.* **1982**, *104*, 6994.

(9) Crabtree, R. H.; Felkin, H.; Morris, G. E. *J. Organomet. Chem.* **1977**, *141*, 205.

(10) Sandstrom, J. *Dynamic NMR Spectroscopy*; Academic Press: New York, 1982.

(film) (cm⁻¹) (mixture of **7Y** and **7H**): 2183, 2233 [m, br, IrH], 3323, 3431 [w, br, NH].

Y = Br⁻. (**7H**) ¹H NMR (CD₂Cl₂) (ppm) at 293 K: -21.9 [1H, td, ²J(PH) = 19.0 Hz, ²J(HH) = 6.2 Hz, IrH], -21.1 [1H, td, ²J(PH) = 19.0 Hz, ²J(HH) = 6.2 Hz, IrH], 5.6–8.4 (34H, m, aromatics and C₅H₄N), 5.2 (2H, s, NH₂). ¹H NMR (CD₂Cl₂) (ppm) at 183 K: (same as that at 293 K except the NH₂ signal) 4.4 (1H, s, NH), 6.2 (1H, s, NH). T_c = 203 K. ³¹P{¹H selectively decoupled} NMR (CD₂Cl₂) (ppm): 18.3 [²J(PH) = 19.0 Hz]. Anal. Calcd for IrP₂N₂BrC₄₁H₃₈: C, 55.10; H, 4.26; N, 3.14. Found: C, 55.00; H, 4.12; N, 3.20. IR (film) (cm⁻¹): 2188, 2232 [m, br, IrH], 3316, 3427 [m, br, NH].

Y = I⁻. (**7H**) ¹H NMR (CD₂Cl₂) (ppm) at 293 K: -22.2 [1H, td, ²J(PH) = 18.2 Hz, ²J(HH) = 5.7 Hz, IrH], -21.1 [1H, td, ²J(PH) = 18.4 Hz, ²J(HH) = 5.7 Hz, IrH], 5.6–8.4 (34H, m, aromatics and C₅H₄N), 5.25 (2H, s, NH₂). ¹H NMR (CD₂Cl₂) (ppm) at 183 K: (same as that at 293 K except the NH₂ signal) 4.5 (1H, s, NH), 6.2 (1H, s, NH). T_c = 208 K. ³¹P{¹H selectively decoupled} NMR (CD₂Cl₂) (ppm): 17.9 [t, ²J(PH) = 18.0 Hz]. Anal. Calcd for IrP₂N₂IC₄₁H₃₈: C, 52.39; H, 4.05; N, 2.98. Found: C, 51.89; H, 4.15; N, 2.54. IR (film) (cm⁻¹): 2191, 2217 [m, br, IrH], 3311, 3417 [w, br, NH].

Y = CN⁻. (**7H**) ¹H NMR (CD₂Cl₂) (ppm) at 293 K: -21.3 [1H, td, ²J(PH) = 15.6 Hz, ²J(HH) = 5.4 Hz, IrH], -21.1 [1H, td, ²J(PH) = 17.4 Hz, ²J(HH) = 5.4 Hz, IrH], 5.6–8.4 (34H, m, aromatics and C₅H₄N), 5.57 (2H, s, NH₂). ¹H NMR (CD₂Cl₂) (ppm) at 183 K: (same as that at 293 K except the NH₂ signal) 4.6 (1H, s, NH), 6.9 (1H, s, NH). T_c = 213 K. ³¹P{¹H selectively decoupled} NMR (CD₂Cl₂) (ppm): 18.2 [t, ²J(PH) = 16.2 Hz]. Anal. Calcd for IrP₂N₃C₄₂H₃₈: C, 60.13; H, 4.53; N, 5.01. Found: C, 59.87; H, 4.76; N, 5.22. IR (film) (cm⁻¹): 2120 [m, CN], 2192, 2204 [w, br, IrH], 3261, 3382 [w, br, NH].

Y = SCN⁻. (**7H**) ¹H NMR (CD₂Cl₂) (ppm) at 293 K: -21.2 [1H, td, ²J(PH) = 14.8 Hz, ²J(HH) = 5.4 Hz, IrH], -20.8 [1H, td, ²J(PH) = 15.4 Hz, ²J(HH) = 5.4 Hz, IrH], 5.6–8.4 (34H, m, aromatics and C₅H₄N), 5.1 (2H, s, NH₂). ¹H NMR (CD₂Cl₂) (ppm) at 183 K: (same as that at 293 K except the NH₂ signal) 3.5 (1H, s, NH), 6.2 (1H, s, NH). T_c = 193 K. ³¹P{¹H selectively decoupled} NMR (CD₂Cl₂) (ppm): 18.3 [t, ²J(PH) = 15.0 Hz]. Anal. Calcd for IrP₂SN₃C₄₂H₃₈: C, 57.91; H, 4.37; N, 5.83. Found: C, 57.83; H, 4.54; N, 5.01. IR (film) (cm⁻¹): 2098 [s, SCN], 2176 [m, br, IrH], 3315, 3403 [m, br, NH].

Dihydrido(acetonitrile)(η^1 -2-aminopyridine)bis(triphenylphosphine)iridium(III) Tetrafluoroborate (8**).** [IrH₂(Me₂CO)₂(PPh₃)₂]BF₄ (20 mg, 0.022 mmol) and 2-aminopyridine (2.1 mg, 0.022 mmol) were dissolved in 5 mL of CH₂Cl₂. CH₃CN (3 μ L) was added to the pale yellow solution, and the mixture was stirred for 5 min. The solvent was removed under vacuum, and the crude solid was recrystallized in 5 mL of CH₂Cl₂-hexane (1:1) to afford [IrH₂(CH₃CN)(pyNH₂)(PPh₃)₂]-BF₄ (**8**) (yield 72%). ¹H NMR (CD₂Cl₂) (ppm) at 293 K: -20.9 [1H, td, ²J(PH) = 16.5 Hz, ²J(HH) = 6.3 Hz, IrH], -20.5 [1H, td, ²J(PH) = 15.6 Hz, ²J(HH) = 6.3 Hz, IrH], 1.70 (3H, s, CH₃CN), 5.8–8.2 (34H, m, aromatics and C₅H₄N), 4.9 (2H, s, NH₂). ¹H NMR (CD₂Cl₂) (ppm) at 183 K: (same as that at 293 K except the NH₂ signal) 4.2 (1H, s, NH), 5.6 (1H, s, NH). T_c = 203 K. ³¹P{¹H selectively decoupled} NMR (CD₂Cl₂) (ppm): 19.5 [t, ²J(PH) = 15.1 Hz]. IR (film) (cm⁻¹): 2176 [m, br, IrH and CN], 3360, 3474 [m, br, NH].

Dihydrido(carbonyl)(η^1 -2-aminopyridine)bis(triphenylphosphine)iridium(III) Tetrafluoroborate (9**).** [IrH₂(Me₂CO)₂(PPh₃)₂]BF₄ (20 mg, 0.022 mmol) and 2-aminopyridine (2.1 mg, 0.022 mmol) were dissolved in 5 mL of CH₂Cl₂. The solution was stirred under CO (1 atm) at room temperature for 5 min. The solvent was removed under vacuum, and the crude solid was recrystallized in 5 mL of CH₂Cl₂-hexane (1:1) to afford [IrH₂(CO)(pyNH₂)(PPh₃)₂]BF₄ (**9**) (yield 69%). ¹H NMR (CD₂Cl₂) (ppm) at 293 K: -18.6 [1H, td, ²J(PH) = 12.9 Hz, ²J(HH) = 2.7 Hz, IrH], -8.1 [1H, td, ²J(PH) = 17.4 Hz, ²J(HH) = 6.3 Hz, IrH], 5.8–7.8 (34H, m, aromatics and C₅H₄N), 4.6 (2H, s, NH₂). ¹H NMR (CD₂Cl₂) (ppm) at 183 K: (same as that at 293 K except the NH₂ signal) 4.0 (1H, s, NH), 5.15 (1H, s, NH). T_c = 213 K. ³¹P{¹H selectively decoupled} NMR (CD₂Cl₂) (ppm): 13.0 [t, ²J(PH) = 14.0 Hz]. IR (film) (cm⁻¹): 2015 [s, CO], 2125 [m, br, IrH], 2181 [w, br, IrH], 3369, 3476 [m, br, NH].

Table 1. Dependence of the **4Y:4H** and **6Y:6H** Ratios on Y (Room Temperature) and Chemical Shifts (δ , ppm) of the H_a Protons

	Y = F ⁻	Y = Cl ⁻	Y = Br ⁻	Y = I ⁻
4Y:4H		0.69	0.14	0
δ_{H_a} (4Y)		11.5	10.5	
δ_{H_a} (4H)		9.5	9.5	9.5
6Y:6H	1	0.49	0.12	0
δ_{H_a} (6Y)	11.9	10.4	8.2	
δ_{H_a} (6H)		8.6	9.0	8.6

Reaction of 3 with HY. **3** (20 mg, 0.028 mmol) was dissolved in 5 mL of CH₂Cl₂, and HY was added (3 μ L; Y = Cl⁻, Br⁻, I⁻). The solution was stirred at room temperature for 5 min, and the solvent was removed under reduced pressure. The crude solid was precipitated in a mixture of CH₂Cl₂-hexane (5 mL; 1:1). The ¹H NMR and ³¹P NMR of the samples so prepared coincide with those obtained for compounds **4H** and **4Y**. Isomer ratios are shown in Table 1.

Computational Method. An effective core potential (ECP) was used for Ir and P. For Ir, the relativistic ECP of Andrae et al. was chosen that includes the 5s and 5p electrons in the valence shell¹¹ along with the accompanying (8s7p6d) Gaussian basis set contracted into [6s5p3d] for the valence shell. For P, a (4s4p) Gaussian basis set contracted into [31/31] with the ECP of Stevens and Basch¹² was selected. For N and C, the (9s5p) primitives of Huzinaga were contracted into the split valence [721/41] of Dunning and Hay.¹³ Both P and N basis sets also included polarization functions (5d/1d and 1d, respectively) to avoid earlier problems with unreasonable calculated metal-ligand bond lengths found when polarization functions were absent. For all hydrogen atoms other than those of PH₃, a (5s) Gaussian basis set of Huzinaga¹⁴ contracted into a [311] basis set and augmented by a (4p/1p) polarization function was used. For H atoms of PH₃, a (4s/1s) basis set was chosen.¹⁵

Structural parameters were optimized by the gradient method at the RHF level with the Gaussian 92 set of programs.¹⁶ The ligands 2-aminopyridine (**L**₁) and formamidine (**L**₂) were optimized with all atoms held planar except the amine hydrogen atoms. For metal complexes, PH₃ was used as a model for the phosphine ligands used experimentally, and only metal-ligand bond distances were optimized within C_s constrained symmetry.

Results and Discussion

2-Hydroxypyridine reacts with IrH₅(PPh₃)₂ in benzene at 80 °C for 15 min to give the air stable chelated species **3**, the identity of which was confirmed by spectral data and a crystal structure. In particular the proton NMR of **3** shows two signals in the hydride region at -21.5 (trans to N) and -29.7 (trans to O) ppm, both showing couplings to two P equivalent nuclei and to one hydride. The ³¹P NMR spectrum consists of a triplet at 22.8 ppm (²J(H,P) = 16.1 Hz).

Reaction of 3 with HY and the Observation of X-H...Y⁻-Ir Hydrogen Bonding. **3** reacts with HY (Y = Cl⁻, Br⁻, and I⁻) to give the halo-hydride species **4** (Y = Cl⁻, Br⁻, I⁻). We ascribe this reaction to protonation at oxygen followed by

(11) Andrae, D.; Haussermann, U.; Dolg, M.; Stoll, H.; Preub, H. *Theor. Chim. Acta* **1990**, *77*, 123.

(12) Stevens, W. J.; Basch, H.; Krauss, M. J. *J. Chem. Phys.* **1984**, *81*, 6026.

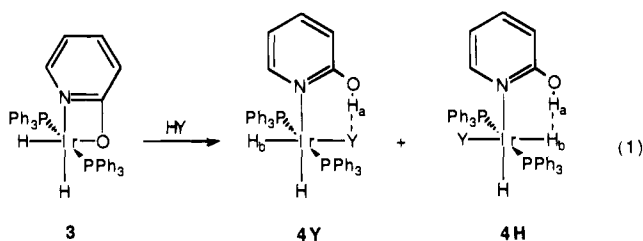
(13) Dunning, T. H.; Hay, P. J. In *Methods of Electronic Structure Theory* 3rd ed.; Schaefer, H. F., Ed.; Plenum Press: New York, 1977; Vol. 1.

(14) Huzinaga, S. *J. J. Chem. Phys.* **1970**, *53*, 2823.

(15) Dunning, T. H. *J. Chem. Phys.* **1965**, *42*, 1293.

(16) Gaussian 92 Revision B: Frisch, M. J.; Trucks, G. W.; Head-Gordon, M.; Gill, P. M. W.; Wong, M. W.; Foresman, J. B.; Johnson, B. G.; Schlegel, H. B.; Robb, M. A.; Replogle, E. S.; Gomperts, R.; Andres, J. L.; Raghavachari, K.; Binkley, J. S.; Gonzalez, C.; Martin, R. L.; Fox, D. J.; DeFrees, D. J.; Baker, J.; Stewart, J. J. P.; Pople, J. A., Gaussian, Inc., Pittsburgh, PA, 1992.

dissociation of the phenolic -OH from the metal, which allows Y to coordinate (see eq 1).



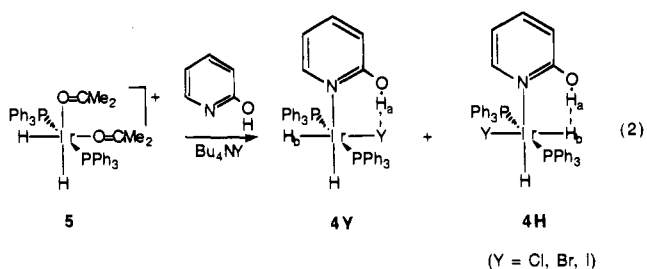
Two isomers are seen for **4**. The evidence suggests these are the **4H** and **4Y** rotamers, in which the OH group hydrogen bonds to the H or Y groups, respectively. As in our previously reported compounds,⁶ H \cdots H coupling is observed for **4H**; indeed the **4H** isomers show the highest H \cdots H coupling that has so far been seen for hydrogen-bonded species (5.5–5.6 Hz). Decoupling of either the hydride or the proton of the ligand clearly shows that they are mutually coupled. The mixture of isomers was unchanged over days at 25 °C.

The OH proton in **4Y** appears 1–2 ppm to low field of its position in **4H**. We assume that this shift of the resonance is due to the H \cdots Y hydrogen bond.¹⁷ On going from Y = Cl⁻ to Y = I⁻, there is a sharp decrease of the **4Y**:**4H** isomer ratio (Table 1), which allows us to establish that the strength of the hydrogen bond decreases in the order H⁻ > Cl⁻ > Br⁻ > I⁻.

On the basis of the T₁(min) value for H_b (82 ms) vs the non-H-bonded hydride proton (242 ms) in compound **4H** (Y = Cl⁻), we can estimate an H_a \cdots H_b distance of 1.7 Å. A similar distance has been estimated in this way for other related compounds.^{5,6}

Addition of CD₃OD to **4** in CD₂Cl₂ led to immediate deuteration of the OH proton of the hydroxypyridine ligand, leading to disappearance of the 5.5 Hz OH \cdots H coupling. Little exchange with any of the hydrides was observed over 4 h, but after 24 h the exchange of both hydrides was complete.

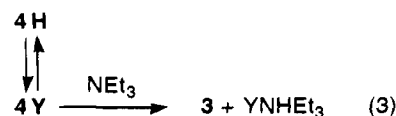
In the case of Y = F⁻, we saw no reaction via eq 1 and considered the possibility that **4** (Y = F⁻) might be accessible by a milder route (eq 2). We find that [IrH₂(Me₂CO)₂-



(PPh₃)₂BF₄ (**5**) reacts with Bu₄NY and 2-hydroxypyridine to give the same mixture of tautomers **4** but only for Y = Cl⁻, Br⁻, and I⁻. In the case of the reaction with Bu₄NF, the cyclometalated species **3** is obtained. We assume that **4** (Y = F⁻) is initially formed but that the complex rapidly loses HF.

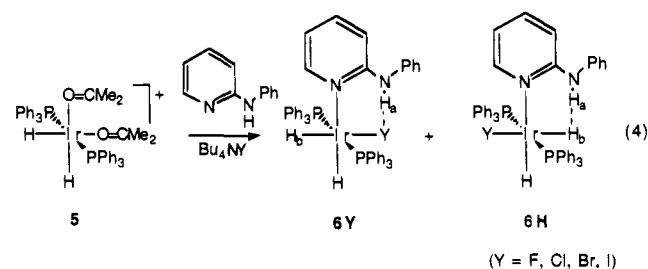
We also obtained the deuterated derivatives of **4H** and **4Y**, IrD₂Y(py-OH)(PPh₃)₂, **4D**, and **4Y-d**, by reacting [IrD₂(Me₂CO)₂(PPh₃)₂]BF₄ with Bu₄NY. The ratio of the isomers having H-bonds to H versus Y (**4D**:**4Y-d**) did not change from that observed for the protonated case **4H**:**4Y**. H-bonds involving H and D are known to have similar energies.^{1a}

Addition of a weak base (NEt₃) to a mixture of **4Y** and **4H** promotes the cyclometalation of the hydroxypyridine ligand, quantitatively yielding compound **3** in 1 min. If NEt₃ promotes the loss of HY from **4Y** (eq 3), then **4H** must convert to **4Y**



before cyclometalation, suggesting that **4Y** and **4H** can exchange on a 1 min time scale. High-temperature ¹H NMR spectra indicate coalescence of the hydride signals of **4Y** and **4H** at 80 °C to give a broad peak at the average chemical shifts, confirming fast exchange.

2-(Aminophenyl)pyridine Complexes. 2-(Aminophenyl)pyridine, (pyNHPh) being less acidic, might be expected to avoid cyclometalation with fluoride. Indeed, when we repeat reaction 2 using pyNHPh and Bu₄NY, we obtain **6**, again as a mixture of isomers **6H** and **6Y** (eq 4). In the case of Y = F⁻,



only compound **6Y** is now formed. In the NMR it shows both a high H \cdots F coupling constant of 65.1 Hz and an N–H proton at low field (11.9 ppm) as expected for N–H \cdots F–Ir H-bonding. The **6Y**:**6H** isomer ratios confirm that the strength of the H \cdots Y hydrogen bond follows the order F⁻ > H⁻ > Cl⁻ > Br⁻ > I⁻ (Table 1).

Addition of CD₃OD to **6** leads to deuteration of H_a. Essentially no exchange of either of the hydrides is observed in ca. 1 h, although equilibrium deuteration is established after ca. 12 h. No H_a \cdots H_b coupling is observed in **6H**, probably due to a decrease of the Ir–H_b basicity in **6H** compared to the trihydride IrH₃(pyNHPh)(PPh₃)₂.^{6b}

2-Aminopyridine Complexes and the H \cdots H Bonds Strength. 2-Aminopyridine is useful in that it allows us to estimate the strength of the H \cdots H hydrogen bond by looking at the coalescence of the two –NH₂ signals in the NMR. From the theoretical studies described below, the rotation barrier in free 2-aminopyridine is very low, ca. 4 kcal/mol. Unfortunately, methylation at the pyridine nitrogen is known to greatly increase this barrier.¹⁸ In IrH₃(pyNHPh)(PPh₃)₂, the pyridine nitrogen is substituted with iridium, and we currently have no unambiguous way of estimating whether this affects the intrinsic rotation barrier. Since the lowest measured barrier in our compounds is 7.6 kcal/mol, this is an upper bound for the intrinsic barrier, which must therefore lie in the range 4–7.6 kcal/mol. In the absence of any better number, we have taken the midpoint of this range, 5.8 kcal/mol as our best estimate for the intrinsic rotation barrier. We therefore identify the H \cdots H hydrogen bond strength with the value obtained by subtracting 5.8 kcal/mol from the observed Ar–NH₂ rotation barrier in the complex, given that the H \cdots H bond is broken in the transition state. We do not regard the absolute value of the H-bond strengths so obtained to be well-determined, because of the assumptions involved; bond strength differences should be reliable, however.

(17) (a) Schneider, W. G. *Hydrogen Bonding*; Pergamon Press: New York, 1959; p 55. (b) Williams, D. H.; Fleming, I. *Spectroscopic Methods in Organic Chemistry*; McGraw-Hill: London, 1966; p 87.

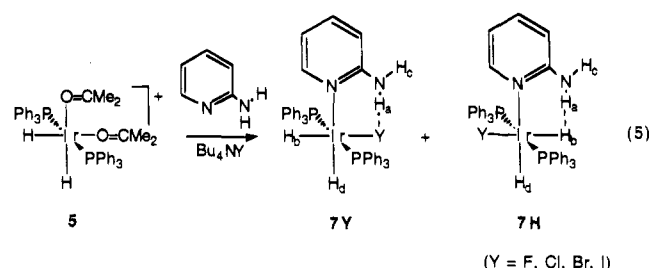
(18) Riand, J.; Chenon, M.-T. *J. Chem. Soc., Perkin Trans. 2* 1987, 1551.

Table 2. Rotational Barriers of the NH₂ Group in **7H**, **7Y**, **8**, and **9** and the Estimated H-Bond Strength of H...H and H...Y Hydrogen Bonds in these Compounds (kcal/mol)^a

	Y = F ⁻	Y = Cl ⁻	Y = Br ⁻	Y = I ⁻	Y = CN ⁻	Y = SCN ⁻	Y = MeCN	Y = CO	Y = H ^{-d}
					H...Y				
rotational barrier	11.0	7.9 ^b	7.6 ^b	<7.1 ^c	<6.9 ^c	<6.0 ^c	<6.6 ^c	<7.2 ^c	
bond strength ^f	5.2	2.1 ^b	1.8 ^b						
					H...H				
rotational barrier	<8.7 ^c	8.7	8.9	9.1	9.2	8.3	8.9	9.5	10.8
bond strength ^f	<2.9	2.9	3.0	3.3	3.4	2.5	3.1	3.7	5.0

^a All values ± 0.2 kcal/mol. ^b Values obtained from the observed **7Y**:**7H** equilibrium ratio (293 K, ¹H and ³¹P NMR). ^c Limiting values estimated considering a maximum of 2% for the undetected isomers at 293 K. ^d Measured for IrH₃(pyNH₂)(PPh₃)₂.^{6b} ^e Assuming an intrinsic C-N rotation barrier of 5.8 kcal/mol (see text).

We synthesized the required compounds from 2-aminopyridine and **5** in the presence of Bu₄NY to give species **7** (Y = F⁻, Cl⁻, Br⁻, I⁻, CN⁻, and SCN⁻). We also prepared some related compounds [IrH₂(L)(pyNH₂)(PPh₃)₂]BF₄ (L = CH₃CN, **8**; CO, **9**) for comparison purposes by methods described in the Experimental Section. Only when Y = Cl⁻ and Br⁻, do we detect a mixture of tautomers at room temperature (eq 5).



For Y = F⁻, only the **7Y** species is detected, while when Y = I⁻, CN⁻, and SCN⁻, only **7H** is observed. Compounds **8** (Y = CH₃CN) and **9** (Y = CO) only showed the N-H...H-Ir interaction (Table 2).

For **4**, **6**, and **7**, addition of CD₃OD leads to deuteration of the ligand OH or NH protons. Only after 24 h is exchange with the hydrides observed, the rate being the same for both IrH groups.

In this system we can measure the strength of the H...H interaction by the NMR method we have previously discussed.⁶ In some cases, we were only able to estimate an upper limit for the strength of the Y...H bond (Y = Cl⁻, Br⁻, I⁻, CN⁻, SCN⁻, CO, CH₃CN), either because the coalescence temperature for the exchange of H_a and H_c in **7Y** was far below the melting temperature of the solvent (CD₂Cl₂; Y = Cl⁻, Br⁻) or because the **7Y** isomer was not detectable at any temperature studied (Y = I⁻, CN⁻, SCN⁻, CO, CH₃CN).

Trans Influence of Y. We find that the Y-Ir-H...H-N bond strength is strongly influenced by the nature of the ligand Y trans to hydride. The strongest A-H...H-Ir bond is formed when Y = H (5.0 kcal/mol), H being the most electropositive element in the series. The weakest H...H bond (<2.9 kcal/mol) is found for Y = F⁻, the most electronegative Y. This is further discussed in the computational section.

Computational Results and Discussion. Before discussing the energetics of the H-bonding interaction, one needs to analyze the geometrical characteristics of this intramolecular interaction, because geometrical constraints might influence the strength of H...H and H...Y bonding. For this purpose a simple geometrical study was performed. The aminopyridine ligand was placed in the IrH₂Y plane, the amino nitrogen was taken as planar, and standard bond distances and angles were assumed. With these constraints, the NH...H-Ir distance is appropriate for H-bonding, but the NH...Y-Ir distances are shorter than the ideal^{1a} distances and the shortening becomes more marked in

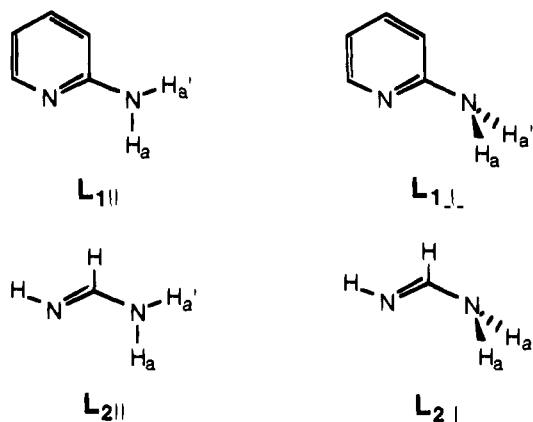
the order F > Cl > Br > I. Even though small structural changes can relieve this shortening to some extent, for example, the energetically facile rotation of bonds such as the Ir-N, we expect the geometrical factor to favor H...H over H...Y hydrogen bonding. In view of the uncertainty of the details of the geometry in the H...Y case, we have only examined the H...H case with ab initio calculations.

The experimentally measured barrier for interchange of the amine hydrogens in IrYH₂(pyNH₂)(PPh₃)₂ results from the preference of the NH₂ unit to remain both planar and in the plane of the pyridine, hereafter called the molecular plane. This barrier comes from two sources: (1) rotation of the C-N bond and (2) breaking of the hydrogen bond between the hydride and amine hydrogen. To evaluate the contribution of each of these factors to the total observed barrier, it was necessary to determine the rotation barrier of free 2-aminopyridine (L₁), of free formamidine (L₂) which we used as a model for coordinated 2-aminopyridine, and then of formamidine bound in the model complex IrH₃(L₂)(PH₃)₂.

Studies of Free Ligands. Free 2-aminopyridine (L₁) was optimized in the two limiting rotational isomers which correspond to the maximum and minimum overlap between the amine nitrogen lone pair and the π system of the pyridine as follows: L_{1||} is the rotamer having the amine nitrogen lone pair parallel to the π system of the pyridine (maximum overlap), and L_{1⊥} is the rotamer having the amine nitrogen lone pair perpendicular to the π system of the pyridine (minimum overlap). L_{1||} was optimized to a structure having essentially no pyramidalization at the amine nitrogen atom; this produces C_s symmetry and a sum of the angles around the amine nitrogen of 360.0°, indicating sp² hybridization at the amine nitrogen atom. This result is in agreement with maximum conjugation between the amine nitrogen and the pyridine ring. In contrast, optimization of L_{1⊥} in constrained C_s symmetry provides a significantly pyramidalized amine nitrogen atom (sum of amine nitrogen angles 323.1°) and a modestly lengthened C-N bond between the pyridine and the amine nitrogen atom (1.43 Å in L_{1⊥} vs 1.37 Å in L_{1||}). These structural changes caused by rotating the amine nitrogen lone pair to a perpendicular orientation with respect to the pyridine π system (L_{1||} to L_{1⊥}) are in agreement with the loss of conjugation upon rotation around the C-N bond. The conjugated system is preferred since L_{1⊥} is found to be 3.70 kcal/mol higher in energy than L_{1||}.

For computational reasons, formamidine (L₂) was used as a model for 2-aminopyridine in the complex. The two limiting rotational isomers of L₂, labeled L_{2||} and L_{2⊥} (corresponding to L_{1||} and L_{1⊥}) were optimized under the same constraints used for L₁.¹⁹ The calculated structural parameters for the forma-

(19) Only the *E* geometric isomer of formamidine was considered here, though formamidine has been thoroughly investigated. For a review see: Hafelinger, G.; Kuske, F. K. H. In *The Chemistry of Amidines and Imidates*; Patai, S., Rappoport, Z., Eds.; Wiley: New York, 1991; Vol. 2, pp 42-100.



midine rotamers are very similar to those calculated for 2-aminopyridine, thus confirming the appropriateness of formamidine as a model for 2-aminopyridine. As this smaller system does not contain an aromatic ring, the barrier to C–N bond rotation is larger and is calculated to be 8.20 kcal/mol. This increase in the calculated rotation barrier is indicative of the increased delocalization of the π system as would be expected for an allylic-type system. This energy difference of 4.50 kcal/mol between the calculated rotation barriers of 2-aminopyridine and formamidine (L_1 vs L_2) necessitates inclusion of a scaling factor between the calculated rotation barriers for the Ir–formamidine complexes and the experimental barriers found for the analogous Ir–2-aminopyridine complexes.

Studies of Ir Complexes. Using the optimized geometry of formamidine, the two metal complexes differing in the position of the amine hydrogen atoms were optimized with constrained C_s symmetry; these complexes are $\text{IrH}_3(L_{2||})(\text{PH}_3)_2$ ($10_{||}$) and $\text{IrH}_3(L_{2\perp})(\text{PH}_3)_2$ (10_{\perp}). There is little variation between the bond lengths calculated for $10_{||}$ and those calculated for 10_{\perp} , but $10_{||}$ is calculated to be 14.42 kcal/mol more stable than 10_{\perp} ; hence, the barrier to rotation of the amine group in the complex $\text{IrH}_3(\text{formamidine})(\text{PH}_3)_2$ is calculated to be 14.42 kcal/mol.

From this calculated rotation barrier, the strength of the $\text{H}_b \cdots \text{H}_a$ interaction can be deduced assuming that only two factors contribute: (1) the loss of amine nitrogen conjugation with the π system upon rotation (i.e., the intrinsic barrier to C–N rotation) and (2) the elimination of the interaction between the hydride and the amine hydrogen upon rotation. In addition, there are two underlying approximations that must be used. First, substitution of PH_3 for PPh_3 will not affect the calculated

rotational barrier. Second, we must assume that binding of 2-aminopyridine (or formamidine) to the Ir does not alter the conjugation between the amine nitrogen and the π system; i.e., the intrinsic barrier to C–N rotation is the same for both coordinated and free 2-aminopyridine (or formamidine). This second assumption is especially important since we will subtract the rotation barrier of the free ligand from the calculated rotation barriers for the Ir complexes to obtain the strength of the H-bond interaction.

Starting with the calculated C–N rotation barrier for $\text{IrH}_3(\text{formamidine})(\text{PH}_3)_2$ of 14.42 kcal/mol, subtracting the 4.50 kcal/mol scaling factor for the difference between formamidine and 2-aminopyridine, the resulting barrier to rotation is estimated to be 9.92 kcal/mol in $\text{IrH}_3(2\text{-aminopyridine})(\text{PH}_3)_2$. This is in close agreement with the experimentally observed rotation barrier of 10.8 kcal/mol, which validates this approach. Further subtraction of the calculated 3.70 kcal/mol intrinsic amine rotation barrier in 2-aminopyridine provides an estimated value of 7.1 kcal/mol for the hydrogen bond between H_b and H_a . Unfortunately, the lack of certainty in the size of the intrinsic barrier to C–N rotation makes comparison of the theoretical and experimental hydrogen bond strengths uninformative.

Examination of the structures and electronic distributions shows that the N–H and Ir–H bonds mutually influence each other (Figure 1). H_b and H_a are close in $10_{||}$ (1.96 Å) but distant in 10_{\perp} (2.58 Å). This change is a result of the rotation around the C–N bond and not of other structural changes around the metal center. The close proximity of the hydric ($\delta^- = -0.26$) H_b and the protonic ($\delta^+ = +0.22$) H_a in $10_{||}$ induces an electrostatic interaction very similar in nature to that of a standard hydrogen bond except for the involvement of hydrogen in both the donor and acceptor and also the nonlinear arrangement of the Ir– H_b and H_a –N vectors. When the geometrical situation is not as favorable to the establishment of the $\text{H}_b \cdots \text{H}_a$ interaction, as in 10_{\perp} , the calculations demonstrate that the negative and positive charges on the respective centers are significantly decreased to levels found in the absence of this interaction ($\delta^- = -0.19$ and $\delta^+ = +0.16$).

The bond orders are also consistent with the presence of an interaction between H_b and H_a since both Ir– H_b and N– H_a Mulliken overlap populations are smaller in $10_{||}$ than in 10_{\perp} . In addition, a very small but positive overlap population, present between H_b and H_a in $10_{||}$ is greatly diminished in 10_{\perp} .

As the ligand *trans* to H_b (Y) was experimentally observed to have an influence on the size of the $\text{H}_b \cdots \text{H}_a$ interaction,

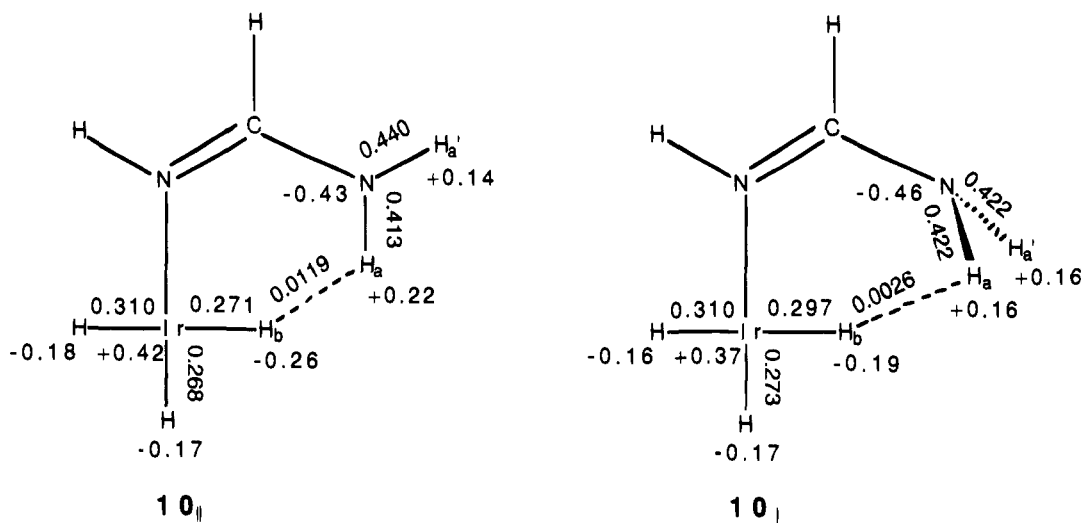


Figure 1.

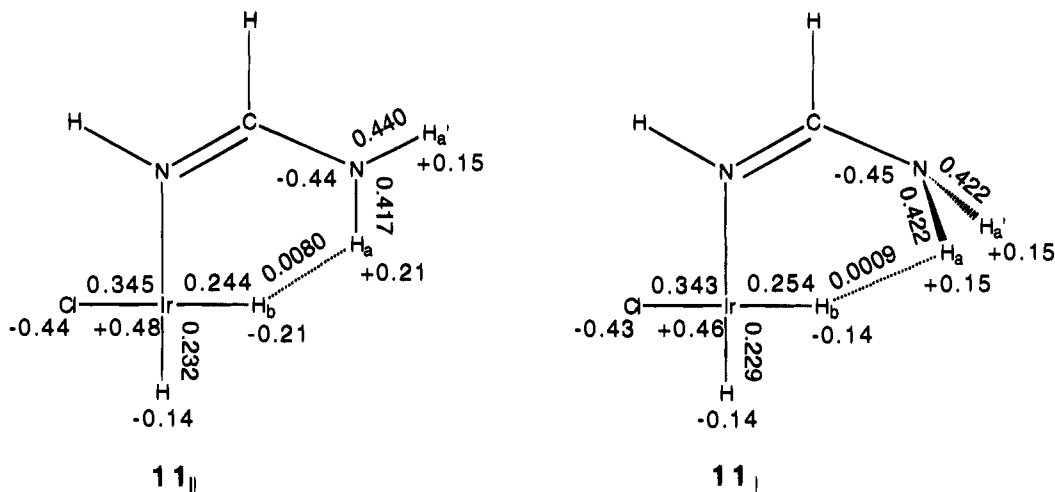


Figure 2.

calculations were also performed on $\text{IrClH}_2(\text{formamidine})(\text{PH}_3)_2$ (**11**) within the same framework described for $\text{IrH}_3(\text{formamidine})(\text{PH}_3)_2$. The barrier to C-N rotation was calculated to be 13.85 kcal/mol which scales down to 9.35 kcal/mol for $\text{IrClH}_2(2\text{-aminopyridine})(\text{PH}_3)_2$ and provides an estimate of 5.65 kcal/mol for the $\text{H}_b \cdots \text{H}_a$ interaction. This decreased interaction when compared to **10** is in agreement with the experimental observations and can be understood in terms of both structural and electronic changes. First, the Ir-H_b distance is shorter by 0.08 Å when trans to chloride instead of hydride due to the weaker σ -donating ability of chloride. This necessarily causes an increase in the $\text{H}_b \cdots \text{H}_a$ separation. In parallel to this increase in distance the charge calculated on H_b diminishes, while the charge calculated for H_a remains unchanged (Figure 2). This suggests that the stronger the trans influence of the ligand opposite to H_b, the greater the $\text{H}_b \cdots \text{H}_a$ interaction. This is in agreement with chemical intuition since a stronger σ donor ligand should weaken the M-L bond trans to it and displace the electronic density toward that trans L ligand.

Conclusion

Intramolecular N-H...H-Ir hydrogen bonding seems to be general and tends to occur whenever a ligand NH bond is suitably placed close to an M-H bond. Hydrogen bonding

between NH and Ir-H is unexpectedly strong for an element having the electronegativity of hydrogen and is of the same order of magnitude as the classical H-bond. It is even stronger than an otherwise analogous N-H...Cl-Ir H-bond in the same system. Only N-H...F-Ir H-bonding is stronger. Several factors have been found to contribute to the strength of the N-H...H-Ir interaction. (1) A favorable geometrical situation allows NH_a and IrH_b to approach very close to one another. (2) The Ir-H_b bond is found to be easily polarized ($\text{Ir}^{\delta+}-\text{H}^{\delta-}$) on the approach of the $\text{N}^{\delta-}-\text{H}_a^{\delta+}$ bond, strengthening the H-bonding interaction with the latter. (3) An increase in the δ^- charge on the hydride resulting from increasing the trans influence of the Y group causes an increase in the H-bond strength. The geometrical situation is not as favorable for N-H...Y-Ir H-bonding (Y = halide) as for the N-H...-Ir case, however.

Acknowledgment. We thank the Ministerio de Educacion y Ciencia (Spain) for a fellowship (E.P.), the Ministère des Affaires Etrangères (France) for a postdoctoral fellowship (J.R.R.), the IDRIS computer center for a generous grant of computer time (O.E.), and the NSF for support (R.H.C. and J.C.L.). The Laboratoire de Chimie Théorique is associated with the CNRS (URA-506) and is a member of ICMO and IPCM.

JA9433683